A NUMERICAL INVESTIGATION OF AN ALPHA STIRLING ENGINE USING THE ROSS YOKE LINKAGE

Iskander Tlili 1*

* Mechanical engineering department, Engineering College, Majmaah University. Kingdom of Saudi Arabia.

E-mail : l.tlili@mu.edu.sa

ABSTRACT

The realization that fossil fuel resources are becoming more and more scarce and considered the largest greenhouse gas emitters and its relationship with climate change, is becoming more pronounced leading to look for adequate strategies concerning energy saving and environmental protection. To achieve this target, much current interest was addressed to Stirling engine since it meets the demands of the efficient use of energy and environmental security. Hence, the development and the investigation about the Stirling engine have come to the attention of many scientific institutes and commercial companies. The engine operates on a closed thermodynamic cycle, which is a regenerative externally heated engine operating with a cycle that has the same thermal efficiency with Carnot cycle if it is ideal and lossless. Several prototypes have already been studied and produced specially gamma and beta configuration. Although the alpha Stirling engine using the Ross Yoke linkage has the advantage of minimizing lateral forces acting on the pistons leading to a more efficient and compact design compared to beta or gamma Stirling configuration, this kind of engine it is not well studied. The objective of this paper was to study the Ross Yoke Stirling engine, which has been developed and validated, by different kind of Stirling engine in order to perform a numerical modelisation of this engine. This model has been used to investigate the effect of the geometrical and physical parameters on Ross Yoke Stirling engine performance in order to determine the significant thermodynamic parameters having an impact on the performance of the engine. As a result, this analysis indicated that the performance of a Ross Yoke Stirling cycle engine with air as working gas depends critically on the heat input and the regenerator effectiveness.

NOMENCLATURE

A	Area	m^2
Cp	Specific heat at constant pressure	$Jkg^{-1}K^{-1}$
Cpr	Heat capacity of each cell matrix	WK^{-1}
Cv	Specific heat at constant volume	$Jkg^{-1}K^{-1}$
d	Hydraulic Diameter	m
D	Diameter	m
ε	Regenerator efficiency	
f_r	Friction factor	
J	Annular gap between displacer and cylinder	m
G	Working gas mass flow	$kgm^{-2}s^{-1}$
k	Thermal conductivity	$Wm^{-1}K^{-1}$
L	Length m	
M	Mass of working gas in the engine	kg
$\dot{m}$	Mass flow rate	kgs^{-1}
m	Mass of gas in different component	kg
P	Pressure	Pa
Q	Heat	J
$\dot{Q}$	Power	W
R	Gas constant	$JkgK^{-1}$
T	Temperature	K
U	Convection heat transfer coefficient	$Wm^{-2}K^{-1}$
V	Volume m^3	
W	Work	J
Z	Displacer stroke	m

SUBSCRIPTS

c	compression space
ch	load
cd	conduction
d	expansion space
E	entered
ext	outside
f	cooler
h	heater
irr	irreversible
moy	*average*
p	Loss
Pa	Wall
pis	piston
r	regenerator
r1	regenerator cell 1
r2	*r*egenerator cell 1
S	left
shtl	Shuttle

GREEK LETTERS

θ	Crank angle	rd
μ	Working gas dynamic viscosity	$kgm^{-1}s^{-1}$
ρ	Density	kgm^{-3}
ω	Angular frequency	$rads^{-1}$
γ	Cp Cv^{-1}	

1. INTRODUCTION

With the rapid development of the global economy, energy requirements have increased notably. The realization that fossil fuel resources required for energy generation are becoming more and more scarce and considered the largest greenhouse gas emitters reported to be the major cause of global warming, has increased interest in seeking alternative options**.** Renewable energy resources are the key to a healthy and sustainable energy future, not only for large-scale energy production, but also for stand-alone systems. Solar energy is one of the more attractive renewable energy sources that can be used as an input energy source for Stirling engine representing one of the most effective applications.

Stirling engines are noteworthy for low pollutant emissions, high efficiency, low noise, minimum vibration, durability, simple construction, ability to self-start, and versatile prime mover for use in such situations as solar thermal generation, micro-cogeneration and other micro-distributed generation situations. Being a regenerative external heated engine with the same theoretical thermal efficiency as Carnot cycle, it uses a wide variety of energy resources such as: solar, waste heat, atomic, geothermal… Although these advantages, none of Stirling engine became competitive with the internal combustion engines, besides its commercial usage was not satisfactory. In fact, different obstacles facing its practical use have been reported in the past such as the lack of sufficiently heat-resistant materials, leakage of working fluid out of the engine, great complexity due to the oscillatory character of the working fluid evolutions, larger volume and mass compared to internal combustion engines and the different varieties of Stirling engine.

These obstacles have actually been reduced due to the high strength of modern materials and alloys, in addition to the development of sophisticated tools of numerical calculation.

Several authors have developed varieties of theoretical and experimental model of Stirling engines, and many prototypes have been designed and built [1-3].

D.G. Thombare et al [4] provided a literature review of the important efforts carried out to develop the Stirling engine cycle and techniques used for engine analysis. They concluded that in order to achieve successful operation of the engine system with good efficiency, a careful design of heat exchangers with a proper selection of the drive mechanism and the engine configuration are crucial. Their study indicated that a Stirling cycle engine working with a relatively low temperature with air as working fluid is potentially the attractive engines of the future, especially solar-powered low-temperature differential Stirling engines with vertical, double acting and gamma configuration.

B. Kongtragool et al [5] designed and constructed a two single-acting, twin power piston and four power pistons with gamma-configuration and low temperature differential Stirling engine. They tested the engine with various heat inputs. The variation of the engine torque, the shaft power and the brake thermal efficiency at various heat inputs with engine speed and performance were presented. They concluded that the engine performance increases while the heat input rises. The engine torque, the shaft power, the brake thermal efficiency, the speed, and the heater temperature also increase with the increasing heat input. Besides, the Beale number of this engine increases in parallel with the decreasing temperature ratio or with the increasing heater temperature.

P. Puech et al [6] conducted a theoretical investigation concerning the thermodynamic analysis of Stirling engine with linear and sinusoidal variations of the volume. They demonstrated that the engine efficiency with perfect regeneration did not depend on the regenerator dead volume. In fact, this latter amplified the imperfect regeneration effect.

S. Wongwises et al [7] carried out a study on the power output determination of a gamma-configuration, low temperature differential Stirling engine. They demonstrated that the mean pressure power formula is most appropriate for the calculation of a gamma-configuration, low temperature differential Stirling engine power output.

B. Cullen et al [8] developed a model for theoretical decoupled Stirling cycle engine used for the analysis of the ideal Stirling cycle engine and its limits on its real-world realization.

H. Karabulut et al [9] conducted an experimental study of a Stirling engine with a lever-controlled displacer driving mechanism charged with helium. He concluded that the effect of charge pressure on the performance characteristics is positive up to a certain value and then negative. The relation between the hot end temperature and the power seems to be linear. For low and moderate heat sources including solar energy, the engine promises a reasonable performance.

F. Formosa et al [10] developed an analytical model for a free piston Stirling engine in order to investigate the effects of the technological and operating parameters on Stirling engine performance. He deduced that the cooler effectiveness affects the engine performances.

Chin-Hsiang Cheng et al [11] developed a numerical model for a beta-type Stirling engine with rhombic- drive mechanism by taking into account different thermal losses. They predict all thermodynamic parameters. They concluded that the performance could be improved by adjusting the influential parameters including the regenerative gap, the distance between the two gears, the offset distance from the crank to the center of the gear, and the heat source temperature.

Halit Karabulut [12] developed a numerical model to study a free piston Stirling engine working with closed and open thermodynamic cycle. He concluded that the power exhibits very big variations with respect to the static position of the piston and the displacer, the hot end temperature, the piston damping coefficient, the displacer rod diameter and the stiffness of the piston spring.

Can Cinar et al [13] carried out an experimental study on a beta-type Stirling engine working at atmospheric pressure. He concluded that an increase in the hot-source temperature leads to an increase in the engine speed and torque and the power-output. Besides, the performance can be increased by using a working fluid with a higher thermal conductivity, such as helium or hydrogen.

All researches concerning Stirling engine are so important, however, there was no sufficient data regarding the best configuration of the Stirling engine models developed in order to calculate and evaluate the optimal design parameters to obtain maximum power and efficiency.

Although the studies were general or focusing on any

available experimental Stirling engine, almost all the results demonstrated that alpha Stirling engine had different advantages compared to beta or gamma Stirling engine. In fact, the alpha Stirling engine especially using the Ross yoke linkage minimizes lateral forces acting on the pistons leading to a more efficient and compact design.
The literature concerning the alpha configuration is so scarce [14] despite the fact that it has many advantages; that is why we were interested in this configuration.

A numerical simulation taking into account different thermal and mechanical losses was developed and tested using different Stirling engines data [15-17]. The results obtained were more realistic than those obtained by other models and correlated closely with the corresponding experimental data. The model was used to determine different thermodynamic parameters of the Ross Yoke Stirling engine in addition to the prediction of the effect of these parameters on the engine performance in order to identify the optimal Thermodynamic parameters.

2. STIRLING ENGINE CLASSIFICATION

2.1. Operating principle

To fulfill thermodynamic Stirling cycle, the engine included two volumes at different temperatures connected to each other through a regenerative heat exchanger and auxiliary heat exchangers.

Originally, Stirling engines were classified into groups according to their geometric configuration. In fact, there are three configuration systems: Alpha, Beta, and Gamma (figure 1).

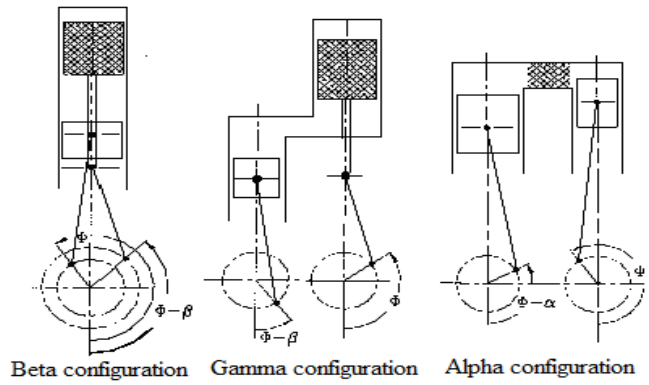

Figure 1: Stirling engine configuration.

These terms described only the Stirling engine cylinder couplings that identified the way in which the displacer piston and the power piston were connected, with respect to the connection of the variable working spaces volume. These are the spaces inside the engine cylinder where the working fluid is heated and cooled respectively in a closed volume.

2.2. The different configurations of Stirling engines

The Beta engine [18] covers the group of Stirling engine using a single cylinder arrangement and where the displacer and the power piston are connected in tandem. The power is produced by the action of the pistons together. This configuration has sealing problems and loses its advantages compared to multi-cylinder engines.

The Gamma engine [19] is very similar to beta-type since the power output is produced in the same manner as in Beta engines. The only difference lies in the fact that the two pistons move in separate cylinders. The disadvantage of this configuration is the large dead space that it has.

The alpha engine [20] consists of two separate cylinders that each one has its own piston, either the displacer or the power piston and three heat exchangers. Each heat source is linked to its own cylinder. The power output is produced by the separate motion of the individual piston.

A rich variety of literature concerning the Stirling engines is available, but no standard terminology concerning the best configuration exists. Most of the literature was published sporadically since 1816 and there were no standardization or clarification of this terminology. This led to rely on diesel engine more than Stirling engine.

Drive mechanisms pose a difficult problem for Stirling engines since discontinuous motion is required to achieve the volumetric changes that result in a net power output [20].

The advantages of Alpha Stirling engine using the Ross yoke linkage (figure 2) are so promoted [20] because of the high power-to-volume ratio, but according to a literature overview, the thermodynamic analysis of this engine was so restricted since it is reported to require high temperature. However, this problem was solved after recent technological advances.

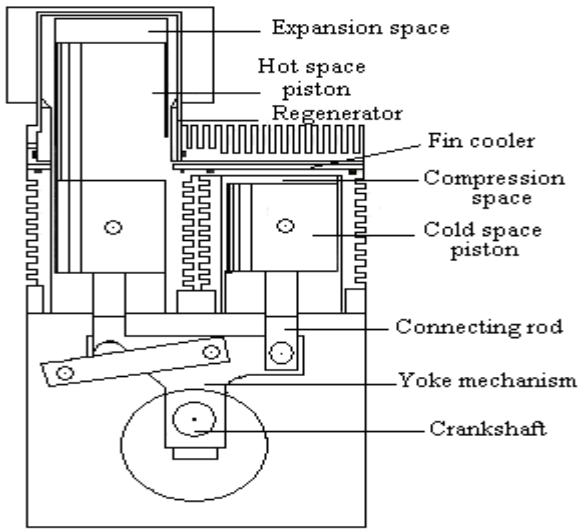

Figure 2: The Ross Yoke drive engine-Schematic cross section view.

3. DESIGN SPECIFICATION AND CONCEPT

3.2. Design concept

The yoke drive mechanism does not produce sinusoidal volume variations and the exact piston displacement functions are extremely complex. The volume variations are derived from geometric considerations in figure 3 and table 1.

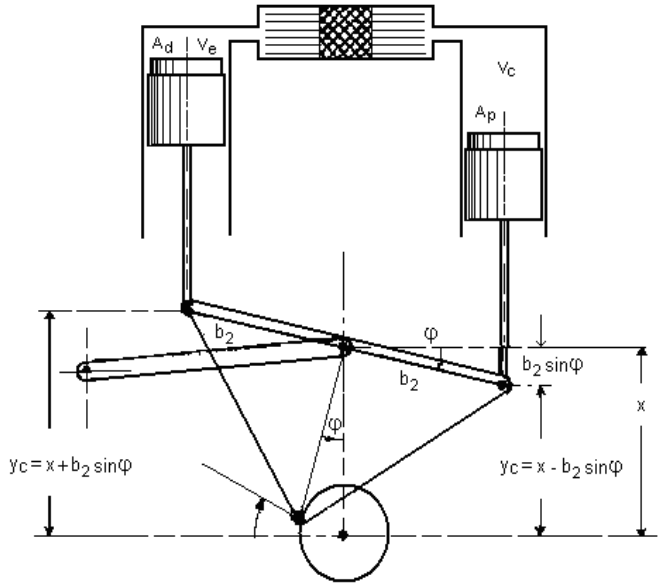

Figure 3: Geometric derivation of the Ross yoke drive equation.

Table 1: Volumes variations.

Geometrical parameters $b_1 \sin\varphi = r\cos\theta$

$$b_\theta = \sqrt{b_1^2 - (r\cos\theta)^2}$$

$$X = r\sin\theta + b_\theta$$

Displacements $Yc = r\,[\sin\theta - \cos\theta\,(b_2 / b_1)\,] + b_\theta$

$Ye = r\,[\sin\theta + \cos\theta\,(b_2 / b_1)] + b_\theta$

Volume variations $Vc = Vmc + Ap\,(Ymax - Yc)$

$Ve = Vme + Ad\,(Ymax - Ye)$

$$\frac{dV_c}{d\theta} = -A_p r\left[\cos\theta + \sin\theta\left(\frac{b_2}{b_1}\right) + \frac{r\sin\theta\cos\theta}{b_\theta}\right]$$

$$\frac{dV_e}{d\theta} = -A_d r\left[\cos\theta - \sin\theta\left(\frac{b_2}{b_1}\right) + \frac{r\sin\theta\cos\theta}{b_\theta}\right]$$

The main Design concepts are listed in Table 2.

Table 2: Concepts and target performance.

Parameters	Values/Type
Engine type	Alpha
Working fluid	Air
Crank length	r = 7.6 mm
Yoke crank length	b1 = 29 mm
Piston length	b2 = 29 mm
Displacement extremities	Ymin = 17.75 mm
	Ymax = 39.28 mm
Swept volumes	Vbc = V mc = 24.42 cm3
Heat exchangers volumes	V_c = 5 cm^3
	V_r = 6.75 cm^3
	V_h = 4.78 cm^3
Mean phase angle advance	α = 90°
Mass of gas in engine	M = 1 g
Hot space temperature	Th = 923 K
Cold space temperature	Tk = 350 K
Frequency	Freq = 41.72 Hz

3.1. Engine specification

The engine parameters should be optimised in order to avoid losses and to obtain high thermal efficiency for all the engine components especially the heat exchangers. While the main target of the engine is to generate sufficient power to run a connecting application, there are conditions which create critical constraints on the design, the working fluid is air and the temperature difference between the heater and the cooler is about 600°C only.

The engine presented in figure 2 uses a Ross Yoke mechanism driving two pistons by the mean of yoke linkage [3]. The major feature of this is that there is almost no lateral movement of the connecting rods resulting in very small side forces on the pistons. With the lack of lateral movement of the connecting rods, there are relatively large unbalanced lateral forces due to the crankshaft counterweight. Ross has a patented gear mechanism which balances the lateral forces by splitting and counter-rotating the counterweight.

In summary, the Ross Yoke is an ingenious mechanism for transferring dual piston motion into rotational motion. It has the advantage of minimizing lateral forces acting on the pistons leading to a more efficient and compact design.

4. ASSUMPTION AND GOVERNING EQUATIONS

There are many different ways to degrade the power produced by an ideal machine and in order to accurately predict the power and the efficiency; a clear understanding of the design compartments is required.

A mathematical model takes into consideration the pressure drop in the heat exchangers [21-24].

Heat transfer and flow friction in the heat exchangers, i.e. the heater, the cooler and the regenerator, are evaluated using empirical equations under steady flow condition.

No leakage is allowed either through the appendix gap or through the seals of the connecting rods.

The temperature distribution in the various engine compartments is illustrated by figure 4.

The gas temperature in the various engine compartments is variable.

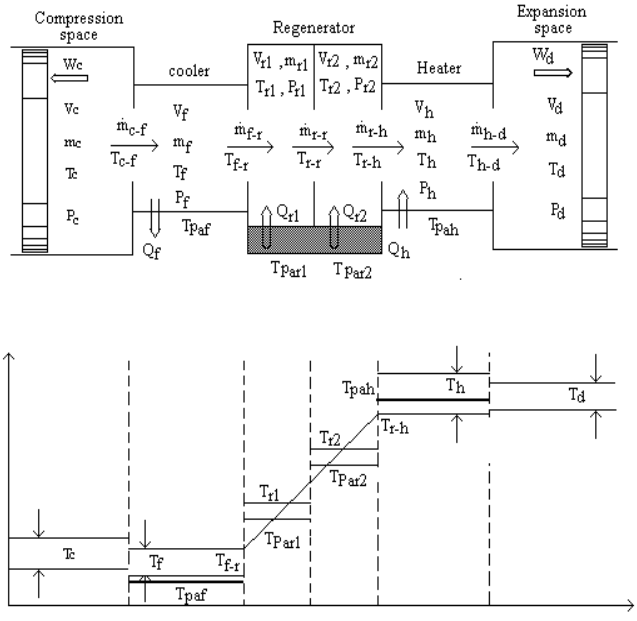

Figure 4: Temperature distribution.

The cooler and the heater walls are maintained isothermally at temperatures Tpaf and Tpah.
The pressure distribution is shown in figure 5.

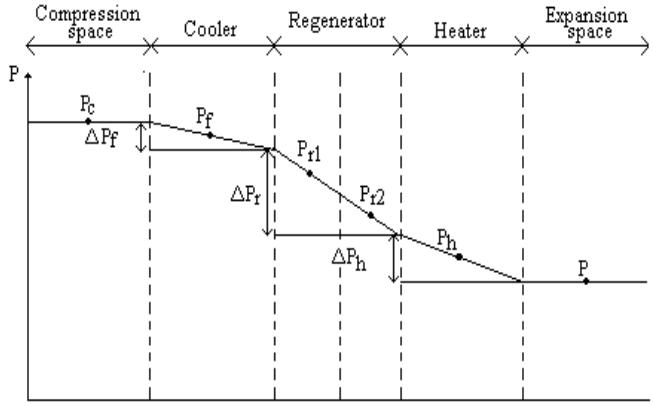

Figure 5 : Pressure distribution.

4.1. Pressure drop in the heat exchangers

Pressure drops due to friction and to area changes in the heat exchangers can easily be modelled using steady flow correlations. These pressure drops lead to a dissipation of work within the heat exchangers leading to a reduction of the available work in the machine.

The frictional drag force is expressed by [25]:

$$F = \frac{2 f_f \, G^2 \, V}{d \rho} \qquad (1)$$

Where G is working gas mass flux ($kg.m^{-2}.s^{-1}$), d is the hydraulic diameter, ρ is gas density ($kg.m^{-3}$), V is volume (m^3) and f_f is the conventional fanning friction factor.

A more suitable definition of the friction factor was proposed by Ureili [3], being so-called 'Reynolds friction factor', as follows:

$$f_r = f_f \, Re \qquad (2)$$

Re is the Reynolds number $Re = \frac{G d}{\mu}$ (3)

The frictional drag force must be equal and opposite to the pressure drop force:

$$F + \Delta p A = 0 \qquad (4)$$

Substituting equation (2) and (3) into Eq. (1) we finally obtain:

$$\Delta p = -\frac{2 f_r \mu G V}{A d^2 \rho} \qquad (5)$$

The internal heat generation which occurs when the gas is forced to flow against the frictional drag force, is given by [26]:

$$\delta \dot{Q}_{Pch} = -\frac{\Delta p \, \dot{m}}{\rho} \qquad (6)$$

$\dot{m}$ is the mass flow rate ($kg.s^{-1}$).

The total heat generated by pressure drop in the different exchangers is:

$$\delta \dot{Q}_{PchT} = \delta \dot{Q}_{Pchf} + \delta \dot{Q}_{Pchr1} + \delta \dot{Q}_{Pchr2} + \delta \dot{Q}_{Pchh} \qquad (7)$$

Where $\delta \dot{Q}_{Pchf}$ is the heat generated by pressure drop in the cooler, $\delta \dot{Q}_{Pchr1}$ is the heat generated by pressure drop in the regenerator r1, $\delta \dot{Q}_{Pchr2}$ is the heat generated by pressure drop in the regenerator r2 and $\delta \dot{Q}_{Pchh}$ is the heat generated by pressure drop in the heater.

4.2. Dynamic model Equations

The gas temperatures in the various compartments are calculated from the perfect gas law:

$$T_c = \frac{P_c . V_c}{R . m_c} \qquad (8)$$

$$T_f = \frac{P_f . V_f}{R . m_f} \qquad (9)$$

$$T_h = \frac{P_h . V_h}{R . m_h} \qquad (10)$$

$$T_d = \frac{P_d . V_d}{R . m_d} \qquad (11)$$

The regenerator is divided into two cells r1 and r2, each cell being associated with its respective mixed mean gas temperature T_{r1} and T_{r2} expressed as follow:

$$T_{r1} = \frac{P_{r1} . V_{r1}}{R . m_{r1}} \qquad (12)$$

$$T_{r2} = \frac{P_{r2} . V_{r2}}{R . m_{r2}} \qquad (13)$$

An extrapolated linear curve is drawn through temperature values T_{r1} and T_{r2} defining the regenerator interface temperature T_{r-f}, T_{r-r} and T_{r-h}, as follows [17]:

$$T_{r-f} = \frac{3T_{r1} - T_{r2}}{2} \qquad (14)$$

$$T_{r-r} = \frac{T_{r1} + T_{r2}}{2} \qquad (15)$$

$$T_{r-h} = \frac{3T_{r2} - T_{r1}}{2} \qquad (16)$$

According to the flow direction of the fluid, the interface's temperatures: T_{c-f}, T_{f-r}, T_{r-h} and T_{h-d} are defined as follows [27]:

If $\dot{m}_{c-f} > 0$ then $T_{c-f} = T_c$ otherwise $T_{c-f} = T_f$

If $\dot{m}_{f-r} > 0$ then $T_{f-r} = T_f$ otherwise $T_{f-r} = T_{r-f}$

If $\dot{m}_{r-h} > 0$ then $T_{r-h} = T_{r-h}$ otherwise $T_{r-h} = T_h$

If $\dot{m}_{h-d} > 0$ then $T_{h-d} = T_h$ otherwise $T_{h-d} = T_d$

Where T_{c-f} is the temperature of the interface between compression space and the cooler, T_{f-r} is the temperature of the interface between the cooler and regenerator, T_{r-h} is the temperature of the interface between the regenerator and the heater, T_{h-d} is the temperature of the interface between the

heater and the expansion space.

The matrix temperatures are thus given by:

$$\frac{dTpa_{r1}}{dt} = -\frac{\delta Q_{r1}}{c_{pr}\ dt} \quad (17)$$

$$\frac{dTpa_{r2}}{dt} = -\frac{\delta Q_{r2}}{c_{pr}\ dt} \quad (18)$$

Where Cpr is the heat capacity of each cell matrix ($J.K^{-1}$), Qr1 is the quantity of heat exchanged to the regenerator r1 (j), Qr2 is the quantity of heat exchanged to the regenerator r2 (j), T_{Par1} is the matrix temperatures in the regenerator r1 (K) and T_{Par2} is the matrix temperatures in the regenerator r2 (K)

By taking into account the conduction loss in the exchangers and the regenerator effectiveness, the power exchanged in the various exchangers is written:

$$\delta\dot{Q}_f = h_f\ A_{paf}\left(T_{paf} - T_f\right) \quad (19)$$

$$\delta\dot{Q}_{r2} = h_{r2}\ A_{par2}\left(T_{par2} - T_{r2}\right) \quad (20)$$

$$\delta\dot{Q}_{r1} = h_{r1}\ A_{par1}\left(T_{par1} - T_{r1}\right) \quad (21)$$

$$\delta\dot{Q}_h = h_h\ A_{pah}\left(T_{pah} - T_h\right) \quad (22)$$

The heat transfer coefficient of exchanges h_f, h_{r1}, h_{r2} and h_h are only available empirically [28].

The total exchanged heat is:

$$\delta\dot{Q} = \delta\dot{Q}_f + \delta\dot{Q}_{r1} + \delta\dot{Q}_{r2} + \delta\dot{Q}_h \quad (23)$$

The work given by the cycle is:

$$\frac{\delta W}{dt} = P_c\frac{dV_c}{dt} + P_d\frac{dV_d}{dt} \quad (24)$$

The thermal efficiency given by the cycle is:

$$\eta = \frac{W}{Q_h} \quad (25)$$

The total engine volume is:

$$V_T = V_c + V_f + V_{r1} + V_{r2} + V_h + V_d$$

The other variables of the dynamic model are given from the energy and mass conservation equation, applied to a generalized cell as follows, (Figure 6):

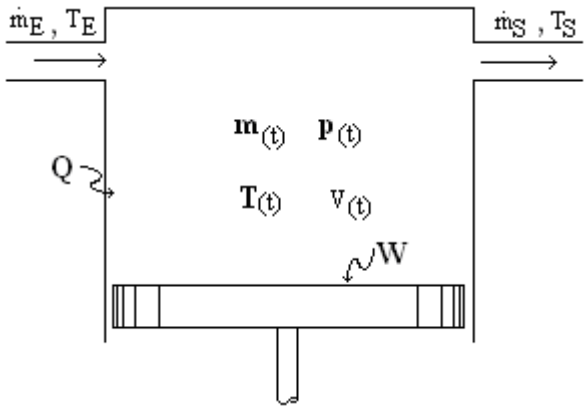

Figure 6: Generalised cell.

- Energy conservation equation [29-31] :

$$\delta\dot{Q} + C_p T_E \dot{m}_E - C_p T_S \dot{m}_S = P\frac{dV}{dt} + C_v\frac{d(mT)}{dt} \quad (26)$$

Since there is a varying pressure distribution throughout the engine, we have arbitrarily chosen the compression space pressure Pc as the baseline pressure. Thus at each increment of the solution, Pc will be evaluated from the relevant differential equation and the pressure distribution determined with respect to Pc. Thus it can be obtained from the following expression:

$$P_f = P_c + \frac{\Delta P_f}{2} \quad (27)$$

$$P_{r1} = P_f + \frac{\left(\Delta P_f + \Delta P_{r1}\right)}{2} \quad (28)$$

$$P_{r2} = P_{r1} + \frac{\left(\Delta P_{r1} + \Delta P_{r2}\right)}{2} \quad (29)$$

$$P_h = P_{r2} + \frac{\left(\Delta P_{r1} + \Delta P_h\right)}{2} \quad (30)$$

$$P_d = P_h + \frac{\Delta P_h}{2} \quad (31)$$

Applying energy conservation equation to the various engine cells, we obtain:

$$-C_p\ T_{c\text{-}f}\ \dot{m}_{cS} = \frac{1}{R}\left(C_p P_c\frac{dV_c}{dt} + C_v V_c\frac{dP_c}{dt}\right) \quad (32)$$

$$\delta\dot{Q}_f - \delta\dot{Q}_{Pchf} + C_p T_{c\text{-}f}\ \dot{m}_{fE} - C_p T_{f\text{-}r}\dot{m}_{fS} = \frac{C_v V_f}{R}\frac{dP_c}{dt} \quad (33)$$

$$\delta\dot{Q}_{r1} - \delta\dot{Q}_{Pchr1} + C_p T_{f\text{-}r}\dot{m}_{r1E} - C_p T_{r\text{-}r}\dot{m}_{r1S} = \frac{C_v V_{r1}}{R}\frac{dP_c}{dt} \quad (34)$$

$$\delta\dot{Q}_{r2} - \delta\dot{Q}_{Pchr2} + C_p T_{r\text{-}r}\dot{m}_{r2E} - C_p T_{r\text{-}h}\dot{m}_{r2S} = \frac{C_v V_{r2}}{R}\frac{dP_c}{dt} \quad (35)$$

$$\delta\dot{Q}_h - \delta\dot{Q}_{Pchh} + C_p T_{r\text{-}h}\ \dot{m}_{hE} - C_p T_{h\text{-}e}\dot{m}_{hS} = \frac{C_v V_h}{R}\frac{dP_c}{dt} \quad (36)$$

$$C_p T_{h\text{-}d} \dot{m}_d = \frac{1}{R}\left(C_p P_d \frac{dV_d}{dt} + C_v V_d \frac{dP_c}{dt} \right) \quad (37)$$

Summing equations (32)-(37) we obtain the pressure variation:

$$\frac{dP_C}{dt} = \frac{1}{C_v . V_T}\left[R(\delta\dot{Q} - \delta\dot{Q}_{PchT}) - C_p \frac{\delta W}{dt} \right] \quad (38)$$

- Mass conservation equation :

$$M = m_d + m_c + m_f + m_r + m_h \quad (39)$$

The mass flow in the various engine compartments are given from the conservation equations of energy (35)-(45):

$$\dot{m}_{cS} = -\frac{1}{RT_{c-f}}\left(P\frac{dV_c}{dt} + V_c \frac{dP_c}{\gamma\, dt} \right) \quad (40)$$

$$\dot{m}_{fS} = \frac{1}{c_p T_{f\text{-}r}}\left(\delta\dot{Q}_f - \delta\dot{Q}_{Pchf} + c_p T_{c\text{-}f} \dot{m}_{fE} - \frac{c_v V_f}{R}\frac{dP_c}{dt} \right) \quad (41)$$

$$\dot{m}_{r1S} = \frac{1}{c_p T_{r\text{-}r}}\left(\delta\dot{Q}_{r1} - \delta\dot{Q}_{Pchr1} + c_p T_{f\text{-}r} \dot{m}_{r1E} - \frac{c_v V_{r1}}{R}\frac{dP_c}{dt} \right) \quad (42)$$

$$\dot{m}_{r2S} = \frac{1}{c_p T_{r\text{-}h}}\left(\delta\dot{Q}_{r2} - \delta\dot{Q}_{Pchr2} + c_p T_{r\text{-}r} \dot{m}_{r2E} - \frac{c_v V_{r2}}{R}\frac{dP_c}{dt} \right) \quad (43)$$

$$\dot{m}_{hS} = \frac{1}{c_p T_{h\text{-}d}}\left(\delta\dot{Q}_h - \delta\dot{Q}_{Pchh} + c_p T_{r\text{-}h} \dot{m}_{hE} \frac{dm_h}{dt}_E - \frac{c_v V_h}{R}\frac{dP_c}{dt} \right) \quad (44)$$

Where: $\dot{m}_{cS} = \dot{m}_{fE}$; $\dot{m}_{fS} = \dot{m}_{r1E}$; $\dot{m}_{r1S} = \dot{m}_{r2E}$; $\dot{m}_{r2S} = \dot{m}_{hE}$ and $\dot{m}_{hS} = \dot{m}_{dE}$

5. METHOD OF SOLUTION

The model developed has been tested using data from the Ross Yoke Stirling engine. This engine has a Ross Yoke linkage system, as shown in Fig. 2. The geometrical parameters of this engine are given in Table 1. The operating conditions are as follows: working gas: air at a mean pressure of 2.195 bar; frequency: 41.72 Hz; hot space temperature: T_{Pah} = 923 K; cold space temperature: T_{Paf} = 350 K.

The independent differential equations obtained in paragraph 4, are solved simultaneously for the variables P_c, m_c, T_{r1}, W, etc. The vector Y denotes the unknown functions. For example, Y_{Pc} is the system gas pressure in the compression space. The initial conditions to be satisfied are noted: $Y(t_0) = Y_0$.

The corresponding set of differential equations is expressed as dY/dt = F(t,Y). The objective is to find the unknown function Y(t) which satisfies both the differential equations and the initial conditions. The numerical solution is composed of a series of short straight-line segments that approximate the true curve Y(t). It starts from the stationary state, with T_c and T_d at T_{Paf} and T_{Pah} or any arbitrary initial temperature values, and goes through successive transient cycles until the values of all the state variables at the end of each cycle are equal to their values at the beginning of that cycle. The system of equations is solved numerically using the classical fourth order Runge–Kutta method, cycle after cycle until periodic conditions are reached.

6. RESULTS AND DISCUSSION

6.1. Pressure variation

The Pressure variation of the model is shown in figure 7. The maximal pressure reached in the engine is of 2.507 bars at the end of the compression phase, and the mean pressure is 2.195 bars.

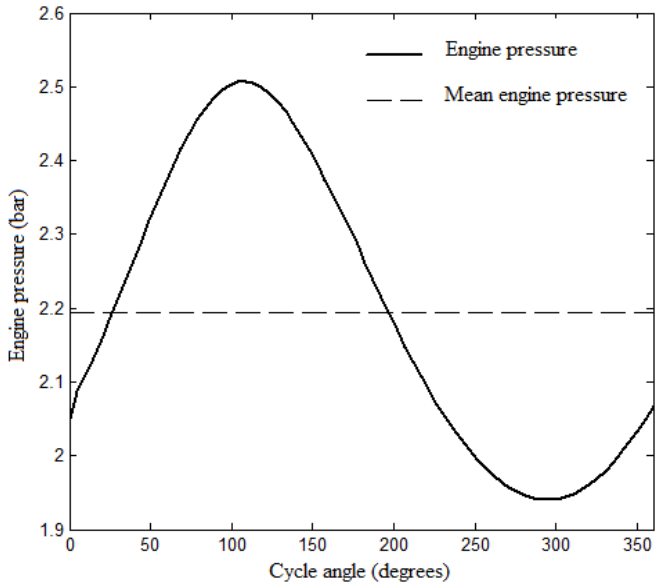

Figure 7: Engine pressure variation.

The surface of the PV diagram shown in figure 8 is equal to the net work produced by the engine.

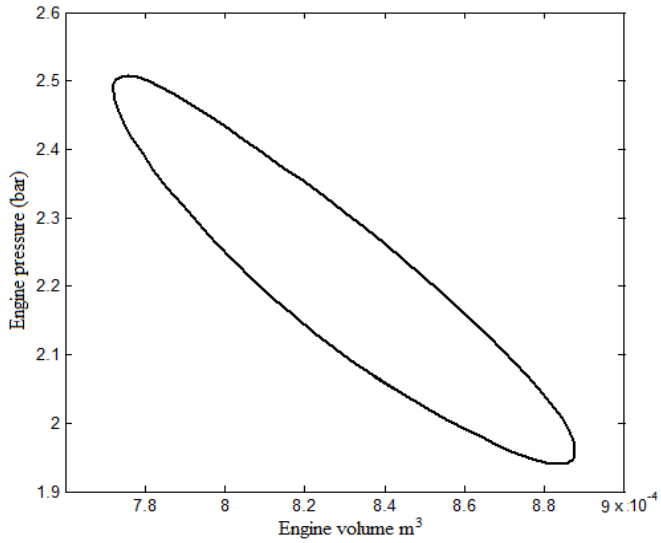

Figure 8: Pressure-volume diagram.

We notice that the work produced in this type of engine and calculated by the dynamic model is lower than that found by the isothermal model since the PV diagram surface is narrowed. This figure shows also the effect of the sinusoidal movement of the displacer piston on P-V diagram.

It is noticed that the average pressure is increased compared to the adiabatic case, due to the effect of temperature variation.

6.2. Temperature variations in different compartment

The temperature variations and the temperature profile of the model are shown in figure 9 and figure 10.

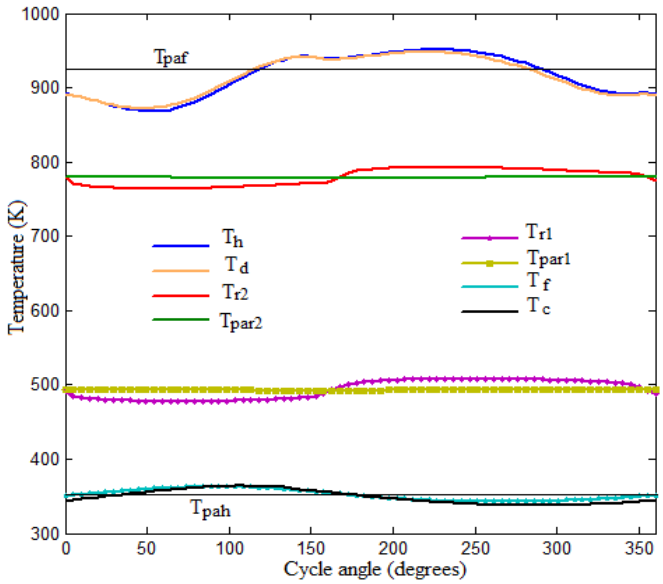

Figure 9: Temperature variations in different compartments.

In the regenerator, we notice that the temperature variation of the matrix (T_{par1}, T_{par2}) is about 10°C which shows that the quantity of heat stored is low. The difference between the matrix and the associated gas temperature (Tr1, T_{r2}) is about 20°C proving that the regenerator has a good effectiveness.

The gas in the heater and the cooler, however, shows a very much higher temperature variation respectively of more than 100°C and 50°C over the cycle.

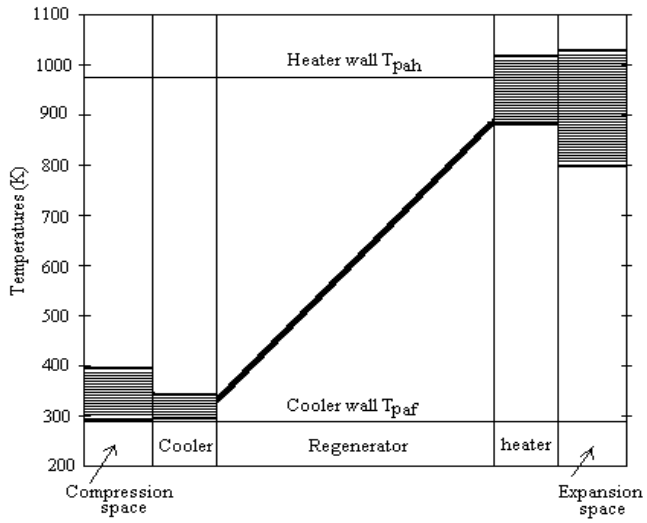

Figure 10: Temperature profile diagram.

The regenerator is one of the most complicated components of the Stirling engine and is the major limiting factor in Stirling engine performance.

6.3. Heat energy and mass flow in different heat exchangers

The heat energy variables Qk, Qr, Qh, and the torque are presented as plots showing the variation of these parameters with the cycle angle in figure (11) and (12).

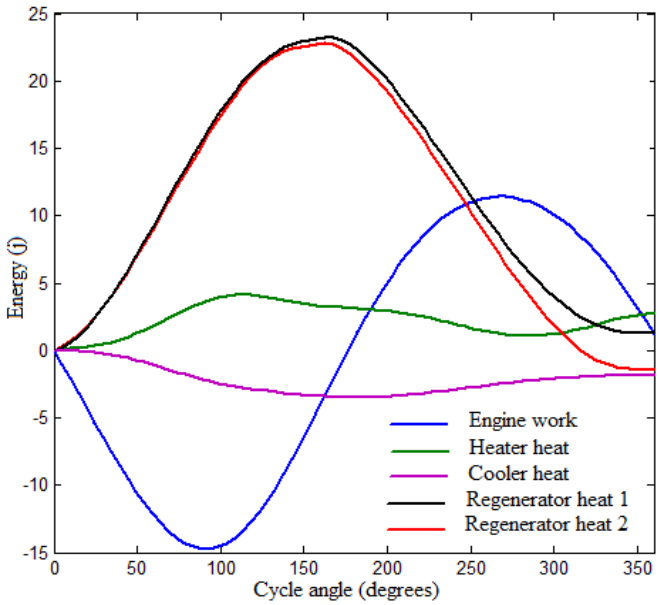

Figure 11: Heat energy variation.

It is noticed that the most significant aspect of the energy-theta diagram is the considerable amount of heat transferred in the regenerator over the cycle, almost ten times than that of the net work done per cycle. This tends to indicate that the engine performance depends critically on the regenerator effectiveness and its ability to accommodate the high heat flow. The energy rejected by the gas to the regenerator matrix in the first half of the cycle is equal to the energy absorbed by the gas from the matrix in the second half of the cycle, which means that the regenerator is properly sized.

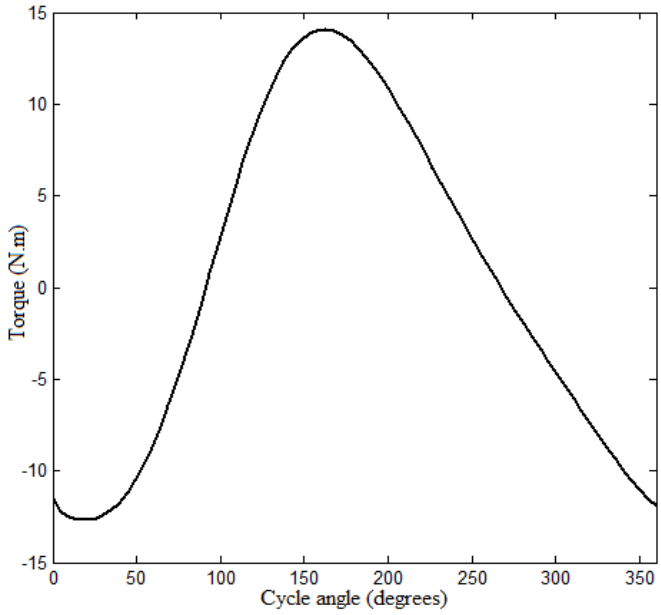

Figure 12: Torque variation.

The corresponding average power is 48.79 W (figure 13). The average heat flow provided by the heater is 118.8 W. The engine effectiveness resulted is up to 41 %. The power and the thermal efficiency calculated by this model are closer to the real power and thermal efficiency of the prototype than other model.

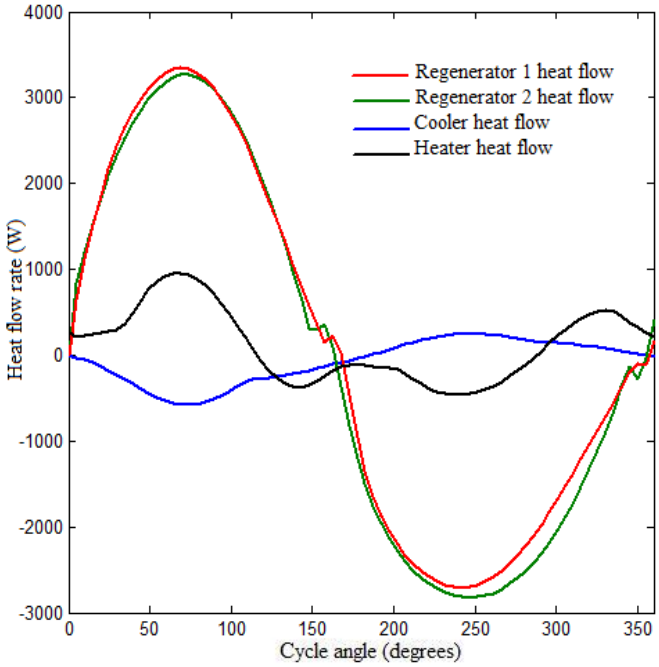

Figure 13: Heat flow variation.

The variation of the mass flow in the different heat exchangers is shown in figure 14. It is noted that the flow in the cooler reaches a value greater than the flow in the regenerator which reaches a higher value than the heater. This is due to the location of the cooler that is close to the engine piston. Besides, we remarked that at the same time the flow can be in the opposite direction, for example when Theta = 150°, the flow is negative in the cooler but positive in the heater.

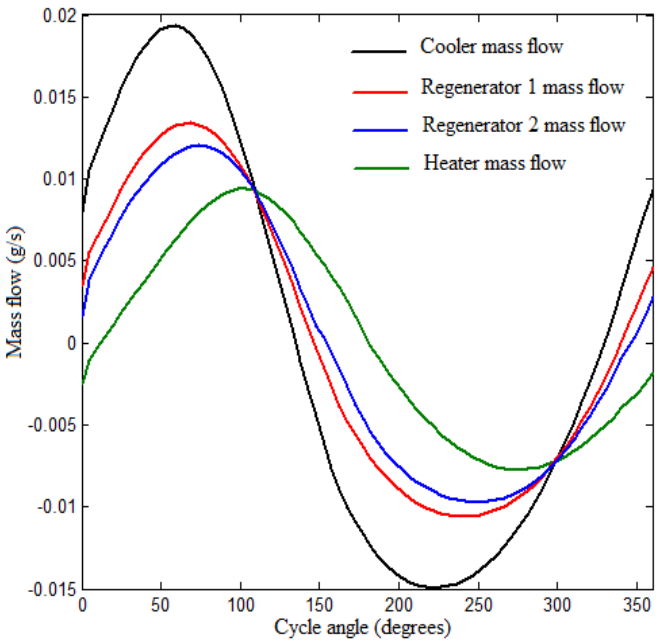

Figure 14: Mass flow variation.

6.4 Pressure drop and energy dissipation in the different heat exchangers

The variation of pressure drop in the heater, regenerator and cooler are shown in figure 15. We Notice that the regenerator is responsible of the undesirable pressure decrease, which attains 0.064 bars because of its geometrical and physical aspects. Whereas the pressure drop in the other exchangers reaches a maximum 0.00268 bar.

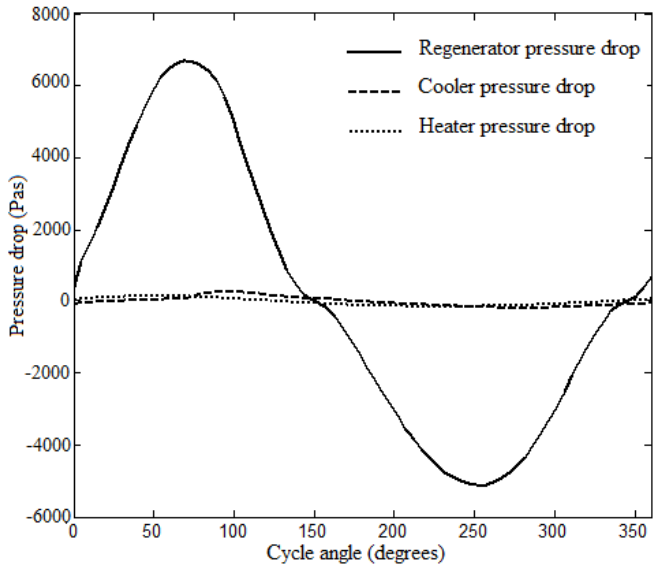

Figure 15: Pressure drop variation.

The energy dissipation in different compartments of the engine is illustrated in the figure 16, Note that the energy dissipation in the regenerator is so high compared to the other exchangers. It is noted that it induces a dissipation of an important energy which reaches a maximum of 80 W while the average is 25 and the engine output is 48.79 W. It is also noticed that approximately 51.24% of power is lost by the regenerator compared to the net power of the engine. Besides, we remark that the power lost by the regenerator is so huge due to its geometrical and physical aspects however its rule is major for the engine output.

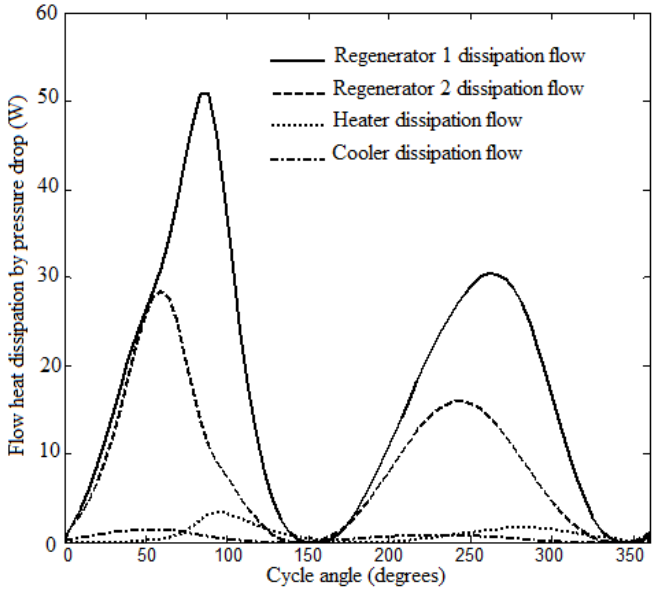

Figure 16: Dissipation flow in different heat exchangers.

6.5 Performance optimization of Ross Yoke Stirling engine

Effect of the fluid mass. An increase of the total mass of gas in the engine leads to a rise in the density, the mass flow, the gas velocity, the load, and pressure function. Therefore, this increase in the total mass of gas in the engine will lead to a more energy loss by pressure drop [15]; however, the engine power increases (figure 17) and the efficiency reaches a maximum of about 42% when the mass is equal to 1 g, as shown in figure 18.

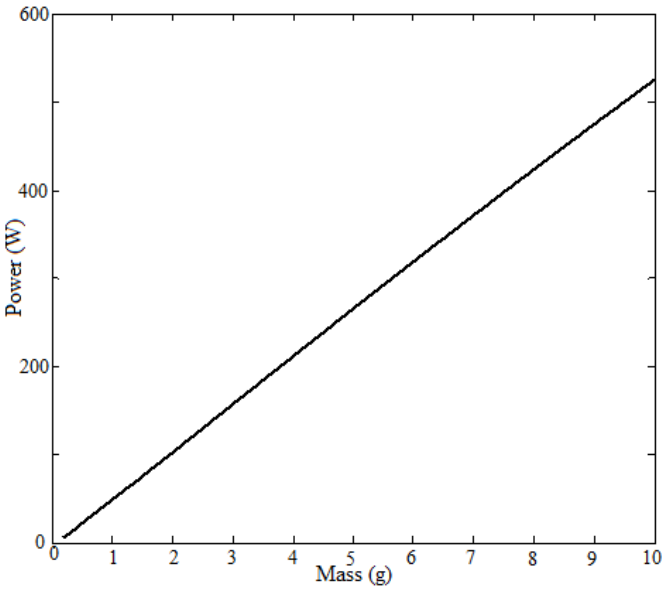

Figure 17: Effect of the fluid mass on the power output.

When the mass increases, the decrease of the efficiency is secondary to an increase of the pressure loss and to the limitation of heat exchanger capacity in the regenerator and the heater. The use of a gas mass equal to 4 g in the engine leads to an acceptable engine efficiency and a higher power than in the prototype.

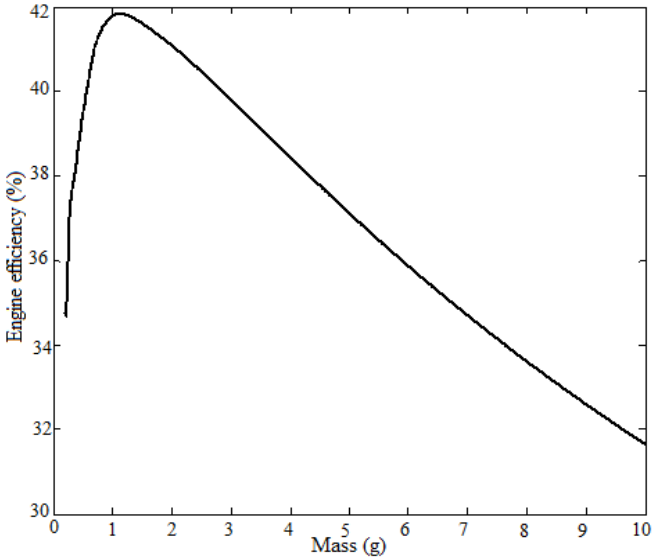

Figure 18: Effect of the fluid mass on the engine efficiency.

We deduce also that the increase of the total mass of gas induces to an incessantly increase in the heat exchanged (figure 19). Besides, it is noticed that when the temperature increases, the heat exchanged augment in parallel.

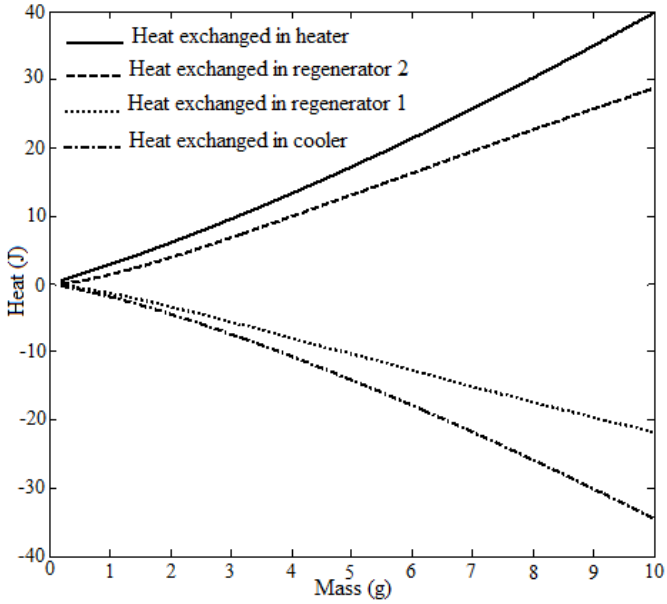

Figure 19: Effect of fluid mass on heat exchanged.

Effect of the heater temperature. Figures (20) and (21) show the effect of the heater temperature on the engine power and efficiency. It is noted that the engine performances increase according to the heater temperature and the power increases in conjunction with the operating frequency.

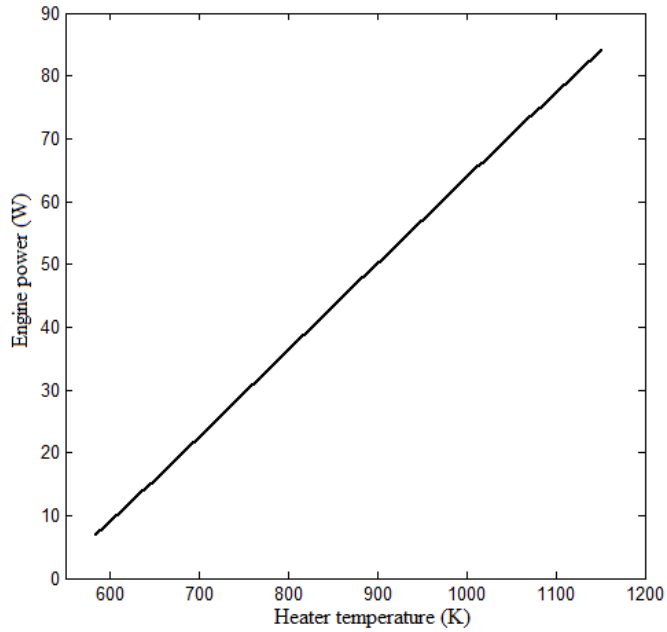

Figure 20: Effect of heater temperature on the power output.

Although the engine losses increase when the heater temperature rises [13], the performances of the engine augment, this is explained by the increase of the exchanged energy between the matrix and the working fluid of the regenerator (figure 22).

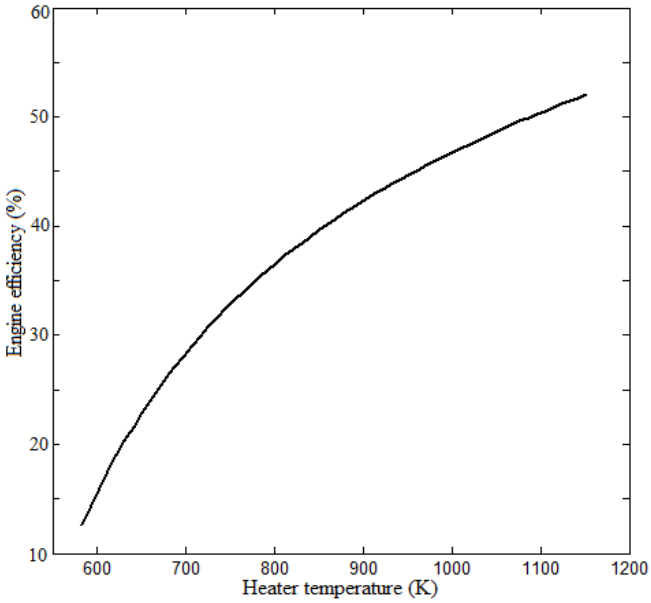

Figure 21: Effect of the heater temperature on the engine efficiency.

The curves indicate that the increase of power with heat source temperature is limitless. Therefore, the progress made in the material technology especially the resistance to high temperature, will improve the performance of Stirling engines.

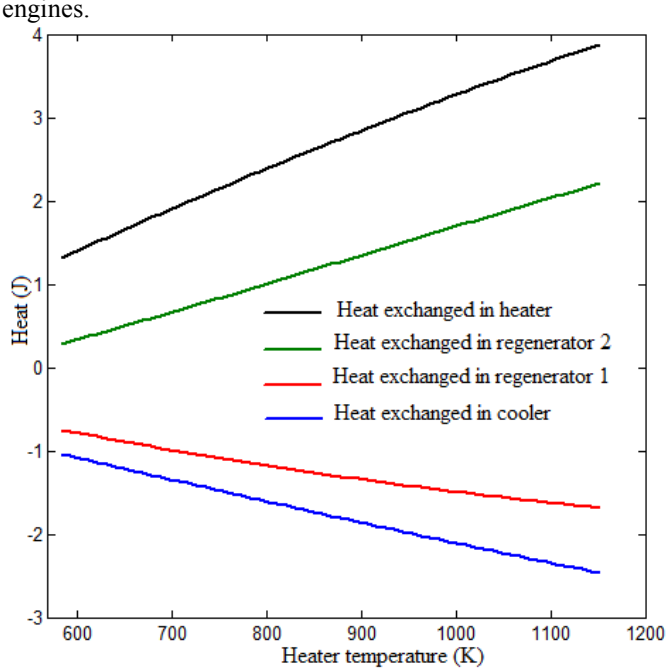

Figure 22: Effect of the heater temperature on the engine efficiency.

We notice also that the increase of the heater temperature induces a continuously increase in the heat exchanged.

Effect of the regenerator volume. The regenerator volume affects the performance of the engine. In fact, the efficiency increases and the engine power reaches a maximum of about 48 W when the volume is equal to 8 10^{-5} m^3, as shown in figure 23 and 24. When the volume increases, the increase of the efficiency is due to an increase of the heat exchanged in the regenerator. The use of a volume equal to 1 10^{-4} m^3 in the engine leads to an acceptable engine efficiency and to a power higher than in the prototype.

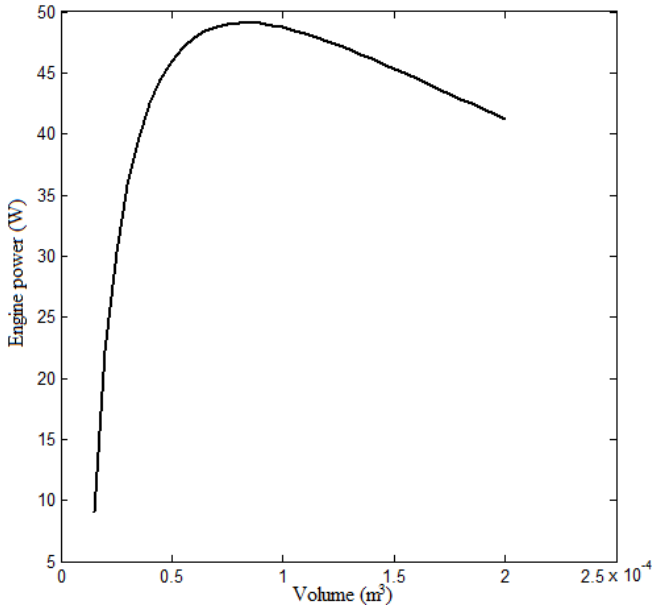

Figure 23: Effect of regenerator volume on the power output

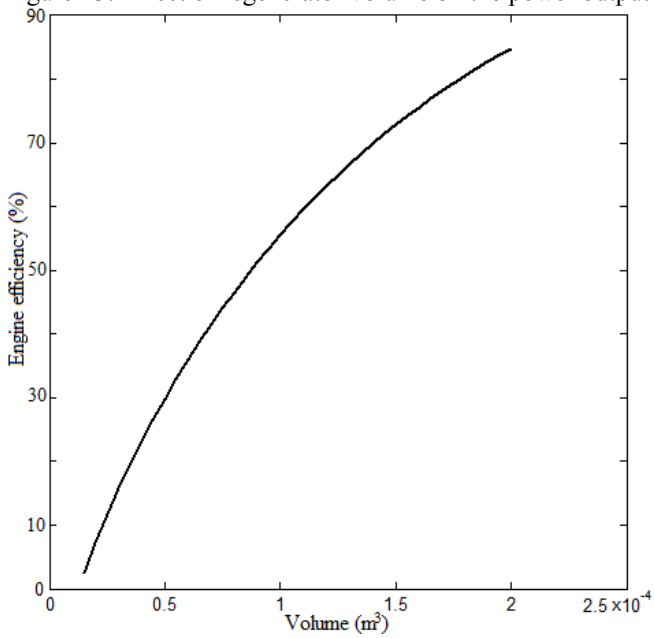

Figure 24: Effect of regenerator volume on the engine efficiency.

Figure 25 and 26 show that the regenerator volume has a very important effect on the heat exchanged in different exchangers. Note that for both the heater and the cooler, the capacity for heat transfer becomes increasingly limited due to an increase in the engine dead volume, whereas the heat transfer increases for the regenerator. It is noteworthy that for a certain value of regenerator volume, the heat exchanged Q_R is null, therefore ,it is considered the optimum volume in which the regenerator takes from the gas the same amount of heat which will be restored.

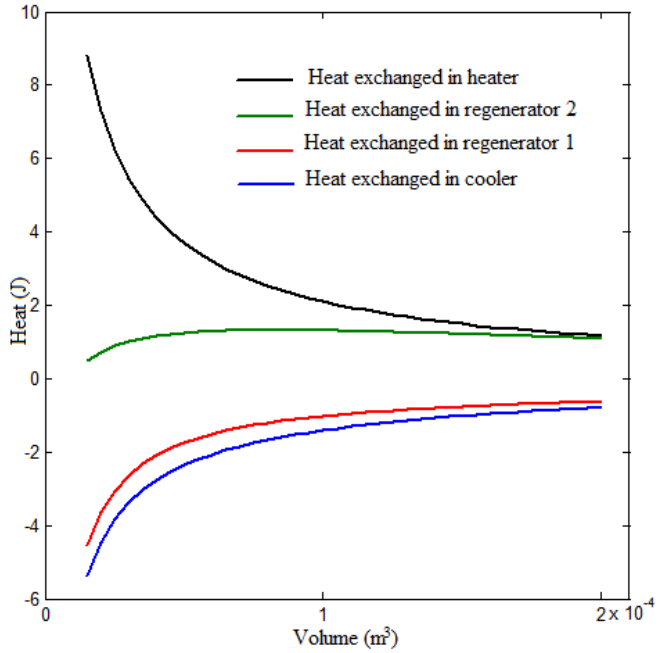

Figure 25: Effect of the regenerator volume on the heat exchanged.

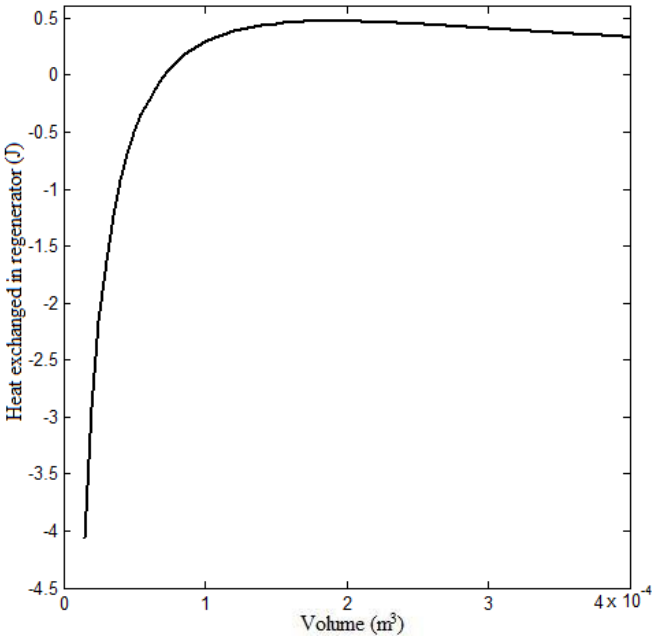

Figure 26: Effect of regenerator volume on regenerator heat exchanged.

7- CONCLUSION

Although the alpha Stirling engine has different advantage compared to beta and gamma Stirling engine and especially when using the Ross Yoke linkage which minimizes the lateral forces acting on the pistons leading to a more efficient and compact design. This kind of engine was not studied enough and effectively, that's why this study was conducted in order to analyze the engine function and identify the most significant parameter affecting its performance.

The numerical model developed and validated with other Stirling engine was applied to Ross Yoke Stirling engine and tested with various thermodynamic parameters.

The following conclusions drawn from this study are:

- Although the regenerator is responsible of the undesirable pressure decrease and all high thermal losses, it remain the most significant compartment of the Stirling engine
- The engine performance depends critically on the regenerator effectiveness and its ability to accommodate the high heat flow.
- Results from this study indicate that the engine performance will increase with the increase of the heater temperature. The engine torque, the heat input, the regenerator heat and the engine efficiency and power increase also in parallel with the increase of the heater temperature. In fact, it can be said that the maximum engine torque, the shaft power, and the brake thermal efficiency increase with the increase of the heat input.
- At a working gas mass equal to 1 g, the engine power increases and the engine efficiency reaches a maximum of about 42%.
- The regenerator volume has a significant effect on the engine performance, the efficiency increases and the engine power reaches a maximum of about 48 W when the volume is equal to 8 10^{-5} $m^{3.}$

The engine performance can be improved by increasing the precision of the engine parts and the heat source efficiency. The engine performance should be increased if a better working fluid e.g. helium or hydrogen is used instead of air.

REFERENCES

1. Walker G. Stirling engines. Oxford: Clarendon Press; 1980
2. James R.-S., Ringbom Stirling engines, Oxford university Press, New York, 1985.
3. I. Urieli, D.M. Berchowitz, Stirling cycle engine analysis, Adam Hilger Ltd, Bristol, 1984.
4. D.G. Thombarea, S.K. Verma, 'Technological development in the Stirling cycle engines', Renewable and Sustainable Energy Reviews 12 (2008) 1–38.
5. B. Kongtragool, S. Wongwises 'Performance of low-temperature differential Stirling engines', Renewable Energy, Volume 32, Issue 4, April 2007, Pages 547-566.
6. P. Puech, V. Tishkova 'Thermodynamic analysis of a Stirling engine including regenerator dead volume', Renewable Energy, Volume 36, Issue 2, February 2011, Pages 872-878.
7. B. Kongtragool, S. Wongwises 'Investigation on power output of the gamma-configuration low temperature differential Stirling engines', Renewable Energy, Volume 30, Issue 3, March 2005, Pages 465-476.
8. B. Cullen, J. McGovern 'Development of a theoretical decoupled Stirling cycle engine', Simulation Modelling Practice and Theory, Volume 19, Issue 4, April 2011, Pages 1227-1234.
9. H. Karabulut, C. Çınar, E. Oztürk, H.S. Yücesu 'Torque and power characteristics of a helium charged Stirling engine with a lever controlled displacer driving mechanism', Renewable Energy, Volume 35, Issue 1, January 2010, Pages 138-143.
10. F. Formosa, G. Despesse 'Analytical model for Stirling cycle machine design', Energy Conversion and Management, Volume 51, Issue 10, October 2010, Pages 1855-1863.
11. C. Chin-Hsiang, Y. Ying-Ju 'Numerical model for

predicting thermodynamic cycle and thermal efficiency of a beta-type Stirling engine with rhombic-drive mechanism', Renewable Energy, Volume 35, Issue 11, November 2010, Pages 2590-2601.
12. H. Karabulut, 'Dynamic analysis of a free piston Stirling engine working with closed and open thermodynamic cycles', Renewable Energy, Volume 36, Issue 6, June 2011, Pages 1704-1709.
13. C. Cinar, S. Yucesu, T. Topgul, M. Okur 'Beta-type Stirling engine operating at atmospheric pressure', Applied Energy, Volume 81, Issue 4, August 2005, Pages 351-357.
14. Kongtragool B, Wongwises S. A review of solar-powered Stirling engines and low temperature differential Stirling engines. Renewable and Sustainable Energy Reviews 2003; 7(2):131–54.
15. Tlili I, Timoumi Y, Ben Nasrallah S, 'Numerical simulation and losses analysis in a Stirling engine, International journal of heat & technology, 2006, Vol. 24, n. 1.
16. I. Tlili, Y. Timoumi, S. Ben Nasrallah. 'Thermodynamic analysis of Stirling heat engine with regenerative losses and internal irreversibilities' Int. J. Engine Res. Vol. 9. p 45-56, 2007.
17. Y. Timoumi, I. Tlili, S. Ben Nasrallah. 'Performance optimization of Stirling engines' Renewable Energy, 2008, 33, 2134–2144.
18. C. Chin-Hsiang, Y. Ying-Ju 'Numerical model for predicting thermodynamic cycle and thermal efficiency of a beta-type Stirling engine with rhombic-drive mechanism', Renewable Energy 2010;35(11):2590e601.
19. R. Gheith, F. Aloui, M. Tazerout, S. Ben Nasrallah 'Experimental investigations of a gamma Stirling engine', Article first published online: Jun 2011, DOI: 10.1002/er.1872.
20. Kolin I., Stirling motor: history-theory-practice, Inter University Center, Dubrovnik, 1991.
21. C. Chin-Hsiang, Y. Ying-Ju 'Combining dynamic and thermodynamic models for dynamic simulation of a beta-type Stirling engine with rhombic-drive mechanism', Renewable Energy, Volume 37, Issue 1, January 2012, Pages 161-173.
22. Curzon FL, Ahlborn B. Efficiency of a Carnot engine at maximum power output. Am J Phys 1975; 43(1):22–4.
23. Jin T. Wang, Jincan Chen ' Influence of several irreversible losses on the performance of a ferroelectric Stirling refrigeration-cycle', 2002, Applied energy 72 495–511.
24. F. Wu, L. Chen, C. Wu, F. Sun, 'Optimum performance of irreversible Stirling engine with imperfect regeneration', Energy Conversion Management Vol. 39, No. 8, pp. 727-732, 1998.
25. S.K. Andersen, H. Carlsen, Per Grove Thomsen. 'Preliminary results from simulations of temperature oscillations in Stirling engine regenerator matrices'. 2005, Energy, p 1–13.
26. Costante M. Invernizzi 'Stirling engine using working fluids with strong real gas effects', Applied Thermal Engineering, Volume 30, Issue 13, September 2010, Pages 1703-1710.
27. I. Batmaz, S. Ustun 'Design and manufacturing of a V-type Stirling engine with double heaters', Applied Energy, Volume 85, Issue 11, November 2008, Pages 1041-1049.
28. M. Abbas, B. Boumeddane, N. Said, A. Chikouche 'Dish Stirling technology: A 100 MW solar power plant using hydrogen for Algeria', International Journal of Hydrogen Energy, Volume 36, Issue 7, April 2011, Pages 4305-4314.
29. Zhaolin Gu, Haruki Sato, Xiao Feng 'Using supercritical heat recovery process in Stirling engines for high thermal efficiency', Applied Thermal Engineering, Volume 21, Issue 16, November 2001, Pages 1621-1630.
30. X.Q. Kong, R.Z. Wang, X.H. Huang. 'Energy efficiency and economic feasibility of CCHP driven by Stirling engine'. Energy Conversion and Management 45, p 1433–1442, 2004.
31. N. Martaj, L. Grosu. 'Exergetical analysis and design optimisation of the Stirling engine'. Int. J. Exergy, 2006, 3(1), 45–66.